

# Recent sex chromosome divergence despite ancient dioecy in the willow *Salix viminalis*

Pascal Pucholt<sup>\*1</sup>, Alison E. Wright<sup>2,3</sup>, Lei Liu Conze<sup>1</sup>, Judith E. Mank<sup>\*2</sup>, and Sofia Berlin<sup>1</sup>

<sup>1</sup> Swedish University of Agricultural Sciences, Department of Plant Biology, Uppsala BioCenter, Linnean Centre for Plant Biology, P.O. Box 7080, SE-75007 Uppsala, Sweden

<sup>2</sup> Department of Genetics, Evolution and Environment, University College London, London WC1E 6BT United Kingdom

<sup>3</sup> Department of Animal and Plant Sciences, University of Sheffield, Sheffield, S10 2TN, UK

\* Corresponding Authors: [pascal.pucholt@slu.se](mailto:pascal.pucholt@slu.se); [judith.mank@ucl.ac.uk](mailto:judith.mank@ucl.ac.uk)

## Abstract

Sex chromosomes can evolve when recombination is halted between a pair of chromosomes, and this can lead to degeneration of the sex-limited chromosome. In the early stages of differentiation sex chromosomes are homomorphic, and even though homomorphic sex chromosomes are very common throughout animals and plants, we know little about the evolutionary forces shaping these types of sex chromosomes. We used DNA- and RNA-Seq data from females and males to explore the sex chromosomes in the female heterogametic willow, *Salix viminalis*, a species with ancient dioecy but with homomorphic sex chromosomes. We detected no major sex differences in read coverage in the SD region, indicating that the W region has not significantly degenerated. However, SNP densities in the SD region are higher in females compared to males, indicating very recent recombination suppression, followed by the accumulation of sex-specific SNPs. Interestingly, we identified two female-specific scaffolds that likely represent W-chromosome-specific sequence. We

show that genes located in the SD region display a mild excess of male-biased expression in sex-specific tissue, and we use allele-specific gene expression analysis to show that this is the result of masculinization of expression on the Z chromosome rather than degeneration of female-expression on the W chromosome. Together, our results demonstrate that insertion of small DNA fragments and accumulation of sex-biased gene expression can occur before the detectable decay of the sex-limited chromosome.

**Key words:** sex chromosomes, masculinization, sex biased gene expression, allele-specific expression

## Introduction

Sex chromosomes are typically thought to diverge as recombination is suppressed between a homologous pair of chromosomes following the acquisition of a sex determination (SD) genetic factor and nearby genes with alleles of sex-specific effects (Bull 1983; Bergero and Charlesworth 2009; Qiu, et al. 2013; Charlesworth 2016; Tennessem, et al. 2016). Sex determination is remarkably variable and a plethora of mechanisms and sex chromosome systems exists (Bull 1983; Bachtrog, et al. 2014). In plants as well as animals, systems can for example either be male heterogametic (females XX, males XY) or female heterogametic (females ZW, males ZZ) (Hodgkin 1990; Goodfellow and Lovell-Badge 1993; Fujii and Shimada 2007; Smith, et al. 2009; Wang, et al. 2012), and both types of systems have evolved many times independently.

The loss of recombination can lead to genetic degeneration of sex-limited W and Y chromosomes (Charlesworth 1996; Papadopoulos, et al. 2015), resulting in functional, structural and transcriptional changes relative to the homologous Z or X chromosome. Over long evolutionary timescales, degeneration can lead to loss of whole chromosomal regions on the non-recombining sex chromosome, making them structurally distinct from the homologous Z or X chromosome, a condition referred to as heteromorphy (Lahn and Page 1997; Carvalho, et al. 2001; Handley, et al. 2004; Papadopoulos, et al. 2015).

However, many organisms with genetic sex determination do not have heteromorphic sex chromosomes. Instead their sex chromosomes are homomorphic

and display limited levels of differentiation, indicating that loss of recombination has not spread very far from the SD locus. Some homomorphic sex chromosomes are old (e.g. European tree frogs (Stöck, et al. 2011), boid snakes (Vicoso, et al. 2013a), emus (Vicoso, et al. 2013b) and ostrich (Yazdi and Ellegren 2014)), however homomorphic sex chromosomes are often evolutionarily young and in the early stage of degeneration, such as in wild strawberry (Spigler, et al. 2008; Tennessen, et al. 2016) and garden asparagus (Telgmann-Rauber, et al. 2007). In some clades, sex determination is extraordinarily dynamic, and closely related species have different SD loci due to rapid and repeated turnover of sex chromosomes across short evolutionary timescales (Phillips, et al. 2001; Miura 2008; Mank and Avise 2009). These turnover events, which are remarkably common in plants and animals (Bachtrog, et al. 2014; Vicoso and Bachtrog 2015), initialize the evolution of novel sex chromosomes and provide a unique possibility for the analysis of the initial steps of sex chromosome evolution.

Even though homomorphic sex chromosomes are common, many questions remain unanswered regarding the evolutionary forces acting on them. Suppression of recombination is thought to arise due to selection for linkage between the SD genetic factor and a nearby mutation with sex-specific effects, i.e. a sexually antagonistic mutation (Fisher 1931; Rice 1996). Once recombination has been halted, a complex suite of sex-specific evolutionary pressures act on the emerging sex chromosomes. Sexually antagonistic mutations are expected to accumulate on the sex chromosomes, and studies of ancient heteromorphic sex chromosomes have shown that male-specific Y chromosomes are commonly enriched for genes with male functions, whereas female-specific W chromosomes are enriched for genes with female functions (Lahn and Page 1997; Carvalho, et al. 2001; Moghadam, et al. 2012). Z (or X) chromosomes can experience accumulation of both male and female beneficial alleles depending on the dominance effects of variation (Rice 1984; Parisi 2003; Emerson, et al. 2004; Wright, et al. 2012; Jaquiéry, et al. 2013). When these mutations are regulatory, sexualization can be evident as an overrepresentation of genes with sex-biased gene expression on the sex chromosomes, which is found in many birds (Wright, et al. 2012; Wang, et al. 2014) and snakes (Vicoso, et al. 2013a). However, it is unclear how quickly the gene content of the sex chromosomes responds to sex-specific selection.

Additionally, following the arrest of recombination, gene expression on the sex chromosomes can also change due to transcriptional decay of the sex-limited W or Y chromosomes. For example, the loss of recombination can lead to genetic degeneration of sex-limited chromosomes (Charlesworth 1996; Papadopoulos, et al. 2015). Moreover, transcriptional degeneration results in reduced expression of the W (or Y) allele compared to the corresponding Z (or X) copy. This process has been shown to occur quickly (Bachtrog, et al. 2008; Papadopoulos, et al. 2015), and we might expect transcriptional decay to precede sexualization, however at this point, it remains unclear whether sexualization precedes or follows transcriptional decay of the sex-limited chromosome.

Willows (genus: *Salix*) and poplars (genus: *Populus*) are woody angiosperms and sister genera in the Salicaceae plant family with substantial levels of genetic divergence in orthologous genes (mean Ka/Ks = 0.33). Most willows and poplars, as well as many other Salicaceae lineages, are dioecious (with male and female flowers on separate plants) (Cronk, et al. 2015), indicating that dioecy evolved early in this clade, more than 45 mya, which is the approximate divergence time of willows and poplars (Boucher, et al. 2003; Manchester, et al. 2006) (fig. 1), although both molecular and fossil estimates contain inherent uncertainty. In plants, initial sex chromosome evolution must follow the transition from hermaphroditism to dioecy, but it is not necessarily expected in all dioecious species. If the evolution of sex chromosomes in willows and poplars coincided with the evolution of dioecy, we would expect conservation of an old sex chromosome system across the group. However, sex chromosomes in both willows and poplars appear to be homomorphic, with the SD locus on chromosome 15 in willows (Hou, et al. 2015; Pucholt, et al. 2015; Pucholt, et al. 2017) and on chromosome 19 in poplars (Gaudet, et al. 2008; Yin, et al. 2008; Pakull, et al. 2009; Paolucci, et al. 2010; Kersten, et al. 2012; Kersten, et al. 2014; Geraldès, et al. 2015), suggesting that the current sex chromosomes evolved independently in each group after the lineages separated (fig. 1). Furthermore, willows studied thus far are female heterogametic (Hou, et al. 2015; Pucholt, et al. 2015; Pucholt, et al. 2017) whereas both female and male heterogamety has been found in poplars (Gaudet, et al. 2008; Yin, et al. 2008; Pakull, et al. 2009; Paolucci, et al. 2010; Kersten, et al. 2012; Kersten, et al. 2014; Geraldès, et al. 2015).

Here we explored the homomorphic sex chromosomes in the willow *Salix viminalis*, a species for which we have previously identified the SD region using

linkage mapping (Pucholt, et al. 2015) and segregation analysis (Pucholt, et al. 2017). We used whole genome and RNA sequencing data from multiple males and females to quantify differences at the sequence and transcriptional levels across the sex chromosomes and autosomes. Our results indicate that the sex chromosomes in this species are very young and have experienced no significant decay in the non-recombinant region. However, despite the recent origin, the Z chromosome has experienced a mild increase in male-biased expression, typically referred to as masculinization of gene expression. This suggests that the unique inheritance of sex chromosomes can produce rapid sex-specific changes in these unique areas of the genome before significant divergence between the sex chromosomes has occurred.

## Results

### *De novo* genome assembly in willows

We sequenced the genomes of two females (ZW) and two males (ZZ) of the female heterogametic willow *S. viminalis* to approximately 30x coverage (approximate genome size 450 Mbp). We then assembled the genome of a male (T76) using SOAPdenovo (Li, et al. 2010), resulting in 78,976 scaffolds longer than 1,000 bp, N50 of 4,291 bp and a total assembly size of 249.8 Mbp. Both diploid willows (*Salix*) and poplars (*Populus*) have a N=19 chromosomes in the haploid phase (Darlington and Wylie 1955) and the chromosomes display conserved synteny over most of their lengths, except for inter-chromosomal rearrangements between chromosomes 1 and 16 (Berlin, et al. 2010; Hou, et al. 2016; Pucholt, et al. 2017). Because karyotypes and synteny are conserved between the two lineages, we used chromosomal information from *Populus trichocarpa* to anchor willow scaffolds, resulting in physical assignment of 13,192 *S. viminalis* genomic scaffolds covering 69 Mbp.

### No large-scale sex chromosome differentiation

We previously identified the SD locus on chromosome 15 by QTL and association studies in two *S. viminalis* bi-parental populations (Pucholt, et al. 2015; Pucholt, et al. 2017), shown in fig. 2A. In order to further characterize the evolution of the sex chromosomes and the SD region, we used genome coverage in females versus males to assess the degree of sequence differentiation between the sex

chromosomes. If Z and W homologous sequences have diverged significantly, mapping efficiencies and genome coverage of Z-linked regions in females will be reduced compared to males, whereas autosomes and the pseudoautosomal region should have equal coverage in both sexes.

In order to assess the level of degeneration, we mapped genomic reads from each male and female individually to our size filtered (scaffolds > 1000 bp) male reference genome. The overall mapping efficiency was high across all individuals ( $70\% \pm 3.6\%$ ) and for scaffolds located on annotated chromosomes (fig. 2B & supplementary fig. S1, Supplementary Material online), including chromosome 15 (fig. 3A), genome coverage was similar between the sexes with only very small variation in coverage between individuals. Reads from both females and males mapped with virtually the same efficiency to the male reference genome (female mapping efficiency =  $71\% \pm 3.1\%$ , male mapping efficiency =  $69\% \pm 5.1\%$ ), indicating that there is no extended female-specific W-linked region.

The insertion of repetitive sequences or major differences in genome size would be predicted to lead to differences in the k-mer profile between males and females. The composition of k-mer frequencies was largely similar between female and male individuals indicating limited degeneration of the W chromosome. The k-mer profiles we observe contain two main peaks reflecting k-mers that are identical in both alleles (high coverage k-mers) and k-mers that originate from only one allele (low coverage k-mers) (supplementary fig. S2, Supplementary Material online). A relatively higher peak for low coverage k-mers reflects a higher heterozygosity of the genome in both males and females. However, the proportion of low coverage k-mers is marginally higher in the male sample (supplementary fig. S2, Supplementary Material online), indicating a higher heterozygosity on a whole genome level compared to the female.

### Small female-specific scaffolds

In order to identify W-specific regions, we performed an *in silico* subtraction by extracting DNA sequencing reads from one of our females that did not map to the male reference genome and assembling them into *de novo* scaffolds. We then remapped reads from both sexes to this female-specific assembly. Of the resulting scaffolds, two exhibited female-limited coverage and were present in both of our females. One scaffold (1,058 bp, supplementary data S1, Supplementary Material online) showed only limited support from one female, with a single read, and

contained no significant hits for any gene found in the NCBI NR database. The second female-specific scaffold (1,948 bp, supplementary data S1, Supplementary Material online) had significant coverage in both female individuals (13.6x and 21.4x coverage) and showed orthology to chromosome 3 in *P. trichocarpa* as well as in the SD region at 10.1 Mbp in chromosome 15 of the *Salix purpurea* genome. Most of the significant hits in the NCBI NR database were genes with unknown function in different species, however some of the hits were annotated as LINE-1 type reverse transcriptase. A domain prediction through the NCBI conserved domains database also showed evidence of a “Non-LTR (long terminal repeat) retrotransposon and non-LTR retrovirus reverse transcriptase (RT)” domain as part of the scaffold.

### **Sequence differentiation in the sex determination region**

Regions which have not diverged sufficiently to exhibit coverage differences may however show elevated SNP density in the heterogametic sex (Vicoso, et al. 2013b) This is because sequence variation can accumulate between the W and Z chromosomes before major W chromosome decay. Therefore, we might expect increased SNP densities in the SD region in females compared to males, whereas SNP densities are expected to be similar between the sexes for autosomes and pseudoautosomal regions.

In line with this prediction, the 82 scaffolds covering 803,676 bp that were linked to the SD region on chromosome 15 are clear outliers for female SNP density relative to the rest of the scaffolds that were located to any position in the genome and males (fig. 2C). The total number of SNPs in the two females in the 82 scaffolds were 9,876 and 10,437, whereas in the two males the corresponding numbers were 6,154 and 5,502. Furthermore the female:male SNP density exceeds the genome-wide 95% confidence interval in the region between 3.5 Mbp and 8.8 Mbp (fig. 3B). Within this region, females have a significantly higher SNP density than in the recombining regions ( $p = 0.004$ , permutation testing, 1000 replicates, supplementary fig. S3, Supplementary Material online) and than males.

We calculated Ks between the male and female genomes in order to estimate divergence between the Z and W chromosomes. The overall genome diversity of the males is reduced in the sex-linked region (Table 1), indicating reduced diversity of the Z chromosome, consistent with the expected drop in effective population size of Z-linked regions (Wright, et al. 2015). Importantly, ZW sex chromosome divergence (in

females) is on the same order as autosomal polymorphism (within 95% confidence interval), implying extremely recent loss of recombination in this region (Table 1). Our SNP analysis thus suggests that recombination has been suppressed very recently on the sex chromosomes of willows, which show significant divergence, but without major W chromosome decay.

Sex chromosomes are expected to evolve more rapidly than autosomes, referred to as Fast-X or Fast-Z evolution (Charlesworth, et al. 1987; Mank, et al. 2010), and Fast-Z evolution has been observed in birds (Mank, et al. 2007a; Wright, et al. 2015), snakes (Vicoso, et al. 2013a) and lepidoptera (Sackton, et al. 2014). In theory, the pattern of Fast-Z accumulates over time, and would be more evident in old sex chromosomes. We therefore tested for Fast-Z evolution in our SD region by comparing average Z-linked and autosomal pairwise Ka/Ks ratios for 16,510 orthologous genes between *S. viminalis* and *P. trichocarpa*. Ka/Ks ratios for Z-linked (mean Ka/Ks = 0.32) and autosomal (mean Ka/Ks = 0.33) genes were not significantly different (t-test,  $p > 0.4$ ), suggesting that a significant Fast-Z effect has not yet occurred in this region (supplementary figure S4, Supplementary Material online).

### **Male-biased expression of sex-like genes in sex determination region in catkins but not in leaves**

Sex chromosomes can be enriched for sex-specific mutations, which often manifests as sex-biased gene expression. In order to quantify the accumulation of sex-biased expression, we assessed mRNA levels for three female and three male distinct and unrelated genotypes from both vegetative (leaves) and sex-specific reproductive (catkins) tissues. We identified 13,987 genes expressed in at least one individual and one tissue. Of these genes, 502 were located on chromosome 15 and 114 were in the SD region.

Based on phenotypic dimorphism in these tissues, we might expect more sex-biased expression in the reproductive catkins than the vegetative leaves. Similar to studies in animals, where the number of sex-biased genes and the average degree of sex-biased expression is far greater in gonadal than somatic tissue (Yang, et al. 2006; Mank, et al. 2007b; Mank 2017), we found more sex-biased genes and greater average sex-biased expression in reproductive (catkin) compared to vegetative (leaf) tissue. This is evident by the far wider sex-bias confidence interval for catkin than leaf

expression (fig 3; supplementary fig. S1, Supplementary Material online), and by the lack of distinct sex-specific clustering of leaf transcriptional profiles (fig. 4). Within the SD region, the overall level of sex-bias in catkins was mildly but significantly male-biased, and exceeded the 95% genomic confidence interval based on sliding window analysis (fig. 3C). However, male-bias in this region was not significantly different from the autosomes based on a binary comparison with permutation testing, likely because many genes in this region are still largely unbiased. In contrast, the sex-bias in the leaves was not significantly different than the 95% confidence interval (fig. 3D).

Male-biased expression in this region could result from two processes that are not necessarily mutually exclusive. The excess of male-biased genes could result from masculinization of the Z chromosome due to accumulation of male-benefit regulatory variation in this region. Alternatively, the decay of W chromosome gene activity would theoretically reduce expression levels in females, and lead to perceived male-biased expression. Degeneration of W-linked sequences would manifest as reduced expression of W-linked alleles relative to the Z-homologs (Bachtrog 2013), in turn producing greater allele-specific expression (ASE) in the SD region in females when compared to either the autosomes and to the males in the same region. We therefore assessed sex-specific ASE by analyzing the abundance of known polymorphisms in RNA-Seq data, i.e. the frequency of the major allele in transcribed RNA at a SNP position detected from DNA data for each individual separately.

Loci in the SD region as well as the autosomes showed variable levels of ASE, however there was no statistical enrichment for ASE in the females in the SD region compared to the autosomes and pseudoautosomal region (Mann-Whitney U-test with Bonferroni correction,  $p > 0.06$  in all individuals), and there was no difference in the SD region between males and females ( $p > 0.9$ , supplementary fig. S5, Supplementary Material online). This suggests that the mild masculinization of the Z chromosome is not due to regulatory decay of the W chromosome, and that the first stages of sexualization of gene content can occur before significant decay of the sex-limited chromosome.

## Discussion

In this work we have studied different evolutionary processes acting in the initial stages of sex chromosome evolution in the dioecious and female heterogametic

willow species *S. viminalis*. The large variation of sex determination systems among species in the Salicaceae plant family indicates the occurrence of one or more recent sex chromosome turnover events (Geraldes, et al. 2015; Pucholt, et al. 2015) and when combined with our data, indicates that the sex chromosomes in this system are extremely young. This is therefore a unique system for studying the processes acting in the early stages of sex chromosomes evolution. To explore these young sex chromosomes, we sequenced the genomes and transcriptomes of *S. viminalis* males and females, in order to assess the level of differentiation between the Z and W chromosomes around the SD locus on chromosome 15. Our results show that mapping efficiency and genome coverage in males and females, a measure of W chromosome differentiation, was not statistically different, indicating that the W chromosome has not significantly decayed around the SD locus (see also Vicoso, et al. (2013a)). These analyses demonstrate that the willow sex chromosomes are to a large degree homomorphic.

It is worth noting that large-scale expansions of low copy and genic sequence on the sex chromosome are unlikely to occur at significant levels in recently evolved sex chromosomes, and instead we might expect repeats would be the major drivers of rapid expansion. However, k-mer abundance profiles of female and male individuals were highly similar, indicating no extensive difference in repetitive sequence content between the genomes. Instead, based on our previous analyses of the SD region in *S. viminalis*, which revealed that recombination in the SD locus was reduced relative to the genome as a whole (Pucholt, et al. 2015), we observe increased SNP density in females, consistent with the accumulation of W-specific SNPs. Transcriptional inactivation of genes on the sex-limited non-recombining sex chromosome has been shown in *Drosophila albomicans* (Zhou and Bachtrog 2012) to happen very early in sex chromosome evolution, and the other plant species thus far assessed have been shown to experience regulatory decay (Hough, et al. 2014; Papadopoulos, et al. 2015). We found, however that allele-specific expression in both females and males in the SD region was not different from autosomal regions, suggesting that regulatory degeneration of the W homolog has not reached discernible levels. Willows therefore show less differentiation than other plants with sex chromosomes, such as *Rumex* (Hough, et al. 2014) and *Silene* (Papadopoulos, et al. 2015).

Even though the W chromosome exhibits no evidence of regulatory decay, we detected mildly significant levels of male-biased expression within the SD region in

reproductive tissue compared to the rest of the genome using our sliding window approach. However, this was not significant using pairwise comparisons, likely because of the wide variance in sex-bias and the large number of unbiased genes in the non-recombining region. Although male-biased expression can result from regulatory decay of the W chromosome, our analysis of allele-specific expression suggests that this is not the case, rather that male-bias results from slight transcriptional masculinization. This is consistent with other Z chromosomes showing evidence of masculinization (Lahn and Page 1997; Carvalho, et al. 2001; Wright, et al. 2012). However, previous evidence of masculinization comes from highly heteromorphic sex chromosome systems, and it was previously unclear how quickly male-biased expression can accumulate on Z chromosome. In contrast, our data suggests that this process can occur rapidly following recombination arrest, and may be one of the first evolutionary signatures to emerge on nascent sex chromosomes. In contrast, we did not observe a significant Fast-Z effect, although this could be influenced by several factors, including overall effective population size and the distribution of fitness effects (reviewed by Meisel and Connallon 2013), and is further complicated by the shared Salicoid polyploidization event which makes the identification of 1:1 willow:poplar orthologs difficult.

Sex-biased expression is thought to result from at least partially resolved sexual conflict (Connallon and Knowles 2005), and the rapid masculinization of gene expression we observe might therefore result from sex-specific functions and sexual conflict. If this is the case, our analysis therefore suggests that there is significant sexual antagonism over optimal expression within the willow transcriptome. However, without comparative transcriptome analysis in related species, we cannot determine whether the SD genetic factor lead to the enrichment of male-biased genes or if the SD genetic factor appeared in an ancestrally male-biased genomic region. Interestingly, this masculinization was confined to reproductive tissue, and corresponding analysis in vegetative leaves revealed marked similarity in gene expression between males and females in this tissue.

The region of elevated female SNP density and sexualized gene expression is evident despite the gaps in coverage in our assembly, suggesting that this region of elevated SNP density could extend somewhat farther along chromosome 15. However, if our sex chromosome boundaries were greater than we detect, we would

expect a larger region of sexualized gene expression. Instead, the areas outside the confidence interval fall within the same 5 Mb region.

Although recombination suppression between Z and W homologs has not progressed very far in the *S. viminalis* SD region, our analyses revealed the presence of short female-specific genomic regions, consistent with W-linkage. Interestingly, sequence similarity of one of these scaffolds shows that it contains a retrotransposon of the LINE-1 type, and shows substantial sequence similarity to *P. trichocarpa* chromosome 3, suggesting potential transposition from chromosome 3 to chromosome 15 the in last common ancestor of willows and poplars. However, without a full assembly of the W chromosome, it is difficult to know the exact evolutionary history of these repeats.

Overall, our results indicate that divergence between the Z and the W homologs in the SD region in willows is very low and recombination ceased very recently, making this an excellent system to study the initial stages of sex chromosome evolution. The enrichment of male biased genes in the SD region as well as insertions of repetitive sequences to the non-recombining sex chromosome are two processes that happens before the decay of the sex-limited chromosome.

## Material and Methods

### Plant Material

Stem cuttings from three *Salix viminalis* female (78021, 78195, 78183) and three male (81084, T76, Hallstad 1-84) accessions, all of them part of the association mapping population described in Berlin, et al. (2014) and Hallingbäck, et al. (2016), were collected from a field archive in Uppsala, Sweden in early spring 2015 and stored in -4°C. The cuttings were transferred to a growth chamber with 22°C constant temperature and 18 h day length to initiate catkin and leaf development. For each accession, fully developed catkins were collected after seven days and young leaves were collected after 13 days. Catkin and leave samples were stored in -70°C awaiting RNA and DNA extraction. Plant material for DNA extraction for two accessions was collected previously by taking stem cuttings from the field archive during winter and growing them in the greenhouse until flowering.

## **RNA and DNA extractions, sequencing, data filtering and k-mer analysis**

Total RNA from the catkins and leaves of all six genotypes was extracted using the Spectrum Plant Total RNA Kit (Sigma-Aldrich Co. LLC) following variant B of the instructions provided by the manufacturer. An on-column DNase treatment step was included. Genomic DNA was extracted from catkins using the DNeasy Plant Mini Kit (Qiagen) following the standard protocol. Library preparations and sequencing was performed by the SNP&SEQ Technology Platform in Uppsala, Sweden. One RNA sequencing library for each accession was prepared from 1 µg total RNA using the TruSeq stranded mRNA sample preparation kit (Cat# RS-122-2101/2102, Illumina Inc.) including polyA selection. The library preparation was carried out according to the manufacturer's protocol (#15031047, rev E). Sequencing was done on an Illumina HiSeq2500 instrument with paired-end 125 bp read length, v4 sequencing chemistry and all twelve libraries were pooled and sequenced on three lanes.

DNA sequencing libraries of four genotypes were prepared from 1 µg of DNA using the TruSeq PCRfree DNA sample preparation kit (cat# FC-121-3001/3002, Illumina Inc.), targeting an insert size of 350-400 bp. The library preparation was performed according to the manufacturer's instructions. Two accessions were sequenced on a lane of Illumina HiSeq2500 with paired-end 125 bp read length (78021 and T76). The other two DNA accessions were sequenced on a lane of Illumina HiSeq2000 with paired-end 100 bp read length (81084 and 78195).

All sequencing data was subsequently processed using cutadapt version 1.9.1 (Martin 2011) and Trimmomatic version 0.32 (Bolger, et al. 2014) to remove adapter sequence and low quality bases and reads containing non determined bases after trimming. Sequencing errors in trimmed DNA sequencing reads were subsequently corrected using lighter version 1.1.0 (Song, et al. 2014) with a k-mer size of 31. Similarly sequencing error in RNA sequencing reads were corrected using Rcorrector (Song and Florea 2015) with a k-mer size of 31. Left over contaminating reads from the PhiX spike in used as internal control in the sequencing process were removed by screening all sequencing reads against the PhiX sequence (RefSeq ID: NC\_001422.1) using bowtie version 1.0.0 (Langmead, et al. 2009).

Trimmed and filtered reads were then analyzed for their k-mer composition using jellyfish version 2.1.4 (Marcais and Kingsford 2011) with k-mer size of 51 bp using the jellyfish packages count and histo.

## Genome assembly and chromosome coordinate assignment

Trimmed and filtered DNA sequencing reads from a single male accession were assembled into genomic scaffolds with SOAPdenovo version 2.04 (Li, et al. 2010) applying default parameters, a k-mer size of 63 and an “expected genome size” of 500 Mbp. The genome size is a rough estimation of an upper bound based on the reported genome size in the related species *P. trichocarpa* (485 Mbp, Tuskan, et al. (2006)) and *S. purpurea* (379-450 Mbp, v1.0, DOE-JGI, [http://phytozome.jgi.doe.gov/pz/portal.html#!info?alias=Org\\_Spurpurea](http://phytozome.jgi.doe.gov/pz/portal.html#!info?alias=Org_Spurpurea)). Only scaffolds larger than 1,000 bp were used in subsequent analyses. The coding sequences of annotated primary transcripts of the *P. trichocarpa* (v. 3.0 - 210) genome were mapped to the scaffolds using nucleotide BLASTn searches (e-value cutoff  $10^{-10}$ ). Only the best BLAST hit per transcript was used; in cases where two best BLAST hits had the same e-value and bitscore, the transcript was discarded. Each scaffold was assigned to the chromosome on which at least 70% of all mapped transcripts agreed. The position of the scaffold in the chromosome was assigned based on the transcripts that mapped to the scaffold.

## Identification of Z-linked sequences from coverage and SNP data

DNA sequencing reads from all individuals were mapped separately back to the genomic scaffolds of the reference individual using the bwa mem algorithm (bwa version 0.7.5, (Li 2013)) and the parameters -A 1 -B 4 -O 6 -E 1 -L 20. Unmapped reads and PCR duplicates were removed using samtools version 0.1.19 (Li, et al. 2009). Reads mapping to multiple positions were filtered out based on the mapping quality of 0. Bedtools version 2.23.0 (Quinlan and Hall 2010) was then used to calculate per site read coverage for every scaffold. An average effective coverage value per scaffold was then calculated as the mean per site coverage of every site in a scaffold that was covered by at least one read. To remove effects of different read depth between individuals the coverage data were normalized for the median coverage value of each individual.

The same mapping files were used to generate nucleotide profiles using the software Sam2Pro (<http://guanine.evolbio.mpg.de/mlRho/>), which were subsequently used for SNP detection. Only sites with a per-site coverage  $\geq 10$  were analyzed. A SNP was called when sites had two bases with a minor allele frequency  $\geq 30\%$ . The average SNP density for every scaffold was calculated as the number of SNPs in a scaffold divided by the number of sites with a per-site coverage  $\geq 10$ , thus correcting for differences in scaffold length. Scaffolds with no such sites were excluded from the analysis. Additionally scaffolds with 100% allele-specific expression values (see below) were excluded from this analysis because such scaffolds are expected to represent missassemblies of merged paralogous genes.

To investigate the regional pattern of the relative female to male SNP density across the genome, a moving average over 25 scaffolds was calculated, and 95% confidence intervals were estimated by bootstrap resampling of mean values of 1,000 random sets of 25 scaffolds. In the bootstrapping process only scaffolds on autosomes were used, all scaffolds located on chromosome 15 were excluded to ensure that the background values were only based on scaffolds not in linkage with the SD locus.

### **Analysis of sex chromosome divergence**

We estimated the time since recombination was suppressed between the Z and W chromosomes using synonymous polymorphism estimates for males and females separately. Based on the identified open reading frame (see above) in the longest isoform of the cufflinks predicted genes, we calculated the number of synonymous sites and the number of synonymous substitutions per gene between the two alleles. In the female SDR the two alleles are expected to represent the homologous genes in the Z and W chromosome. Sites were filtered for a minimum of 10X coverage. Triallelic sites (third allele  $>10\%$ ) were excluded and a minor allele frequency  $> 30\%$  used in SNP calling. We summed the number of synonymous polymorphisms and sites across the SD region and autosomes for males ( $p_i s_m$ ) and females ( $p_i s_f$ ) separately.

### **Analysis of Fast-Z effect**

To analyze the Fast-Z effect we identified the longest isoform for all genes predicted by cufflinks and the orthologous gene in the primary *P. trichocarpa* transcriptome as reciprocal best BLAST hit (e-value  $< 10^{-10}$ ). After identifying open reading frames based on the *P. trichocarpa* protein sequence we used PRANK

(Löytynoja 2014) to align the coding sequences. Gaps were removed from the alignment and codeml in PAML (Yang 2007) (runmode -2) was used to calculate Ka/Ks, Ka and Ks for all alignments of more than 100 bp length. Orthologs with a low number of synonymous substitutions ( $S^*Ks < 1$ ) and with a  $Ks > 2$  (Axelsson, et al. 2008) were removed and we then used a t-test to asses if the Ka/Ks value of genes within the SD region is different from that of genes on the autosomes. Additionally, the distribution of Ka/Ks values was plotted as a histogram.

### Assembly of female-specific scaffolds

All reads pairs originating from one female individual that did not map to the male reference genome assembly were extracted from the read file and used in a new *de-novo* assembly in SOAPdenovo with identical parameters as for the male assembly. Subsequent DNA sequencing reads from all individuals were mapped separately back to the genomic scaffolds of this female-specific assembly using the same bwa mem parameters as before and the per scaffold read coverage was calculated as detailed above. Scaffolds that were female-limited in coverage with coverage in both female accessions were identified, and BLASTed against the *P. trichocarpa* genome sequence version 3.0 ([https://phytozome.jgi.doe.gov/pz/portal.html#!info?alias=Org\\_Ptrichocarpa](https://phytozome.jgi.doe.gov/pz/portal.html#!info?alias=Org_Ptrichocarpa)) and *S. purpurea* genome sequence version 1.0 DOE-JGI ([http://phytozome.jgi.doe.gov/pz/portal.html#!info?alias=Org\\_Spurpurea](http://phytozome.jgi.doe.gov/pz/portal.html#!info?alias=Org_Spurpurea)). Data on potential function of genetic elements in the scaffolds was extracted from a BLASTx search against the NCBI NR protein database (<http://blast.ncbi.nlm.nih.gov/Blast.cgi>) and functional domains were detected by querying the NCBI Conserved Domain Database (Marchler-Bauer, et al. 2015).

### Transcriptome assembly and analyses of sex biased gene expression

Transcripts in the genomic scaffolds were assembled following the Tophat/Cufflinks approach. RNA-seq reads from all genotypes and tissues were mapped separately to the genomic scaffolds using tophat version 2.1.1 (Kim, et al. 2013) with an expected insert size of 200 bp. Cufflinks version 2.2.1 (Trapnell, et al. 2010) was used with default settings to detect transcripts, merge them to a consensus transcriptome for all samples and calculate expression values separately for each sex and tissue. The three unrelated genotypes of each sex were treated as biological

replicates. Genes were only included in the analysis if they were expressed above FPKM = 1 in at least 50% of the individuals. Filtering was done separately for leaves and catkins.

Relative female to male expression was first calculated per gene and a moving average over 25 genes was then used to analyze variation in sex biased expression across the genome. 95% confidence intervals were estimated by bootstrap resampling of mean values of 1,000 random sets of 25 genes for both tissues separately. In the bootstrapping process genes located on chromosome 15 were excluded to ensure that the 95% confidence intervals were only based on genes not in linkage with the SD locus. To analyze tissue-specific expression patterns we generated a heatmap of expression values for all individuals and tissues. In the analysis we used all genes that were expressed significantly sex-biased in at least one tissue ( $\log_2$  fold change  $> 1$  and q value (FDR)  $< 0.05$ ) and that were expressed on average at least with a FPKM value of  $> 1$  in all sex/tissue combinations. Samples were clustered using hierarchical cluster analysis on the pairwise Euclidian distance.

### **Allele-specific expression**

For each genomic SNP identified from the whole genome DNA sequencing, the relative expression of minor and major allele in each individual was quantified using RNA-seq data. To ensure that the coverage values for DNA and RNA are comparable, nucleotide profiles for RNA data were calculated based on mapping with bwa mem with the same parameters as stated above for DNA sequencing. Only SNPs within exons predicted by cufflinks (see above) with  $\geq 10$  mapped RNA reads were included in the analysis. Allele-specific expression (ASE) of all genes was calculated as the median value of the major allele frequency of all SNPs within the gene. In some cases all RNA reads appeared to originate from one allele, however such genes had high SNP density based on the DNA data and we assume that they reflect cases of misassembly of two paralogous sequences together. ASE in such cases reflects paralog-specific expression. We therefore removed all genes with a “major allele frequency” of 100% from the analyses.

The allele specificity of gene expression was then compared between the SD region and the autosomes for all tissues and individuals separately using a Mann-Whitney U Test on the distribution of the major allele frequency of all genes in the

SD region compared to the major allele frequency of all genes on the autosomes. The p values were adjusted using the method of Bonferroni.

## Data Availability

The sequence data have been deposited at the European Nucleotide Archive (ENA) with the accessions PRJEB15049 (genomic sequences) and PRJEB15050 (RNA sequences).

## Supplementary Material

Supplementary figures S1 – S5 and supplementary data S1 are available at Molecular Biology and Evolution online (<http://www.mbe.oxfordjournals.org/>).

## Acknowledgements

We thank four anonymous reviewers and the associate editor Stephen Wright for their insightful suggestions during the editorial process. Sequencing was performed by the SNP&SEQ Technology Platform in Uppsala, Sweden. The facility is part of the National Genomics Infrastructure (NGI) Sweden and Science for Life Laboratory. The SNP&SEQ Platform is also supported by the Swedish Research Council and the Knut and Alice Wallenberg Foundation. This work was supported by the Swedish Research Council (Vetenskapsrådet, VR) (Project grant 2011-3544), the Helge Ax:son Johnsons Foundation, and the European Research Council (grant agreements 260233 and 680951).

## References

- Axelsson E, Hultin-Rosenberg L, Brandstrom M, Zwahlen M, Clayton DF, Ellegren J. 2008. Natural selection in avian protein-coding genes expressed in brain. *Mol Ecol* 17:3008-3017.
- Bachtrog D. 2013. Y-chromosome evolution: emerging insights into processes of Y-chromosome degeneration. *Nat Rev Genet* 14:113-124.
- Bachtrog D, Hom E, Wong KM, Maside X, de Jong P. 2008. Genomic degradation of a young Y chromosome in *Drosophila miranda*. *Genome Biol* 9:R30.
- Bachtrog D, Mank JE, Peichel CL, Kirkpatrick M, Otto SP, Ashman T-L, Hahn MW, Kitano J, Mayrose I, Ming R, et al. 2014. Sex determination: Why so many ways of doing it? *PLoS Biol* 12:e1001899.

- Bergero R, Charlesworth D. 2009. The evolution of restricted recombination in sex chromosomes. *Trends Ecol Evol (Amst)* 24:94-102.
- Berlin S, Lagercrantz U, von Arnold S, Öst T, Rönnberg-Wästljung AC. 2010. High-density linkage mapping and evolution of paralogs and orthologs in *Salix* and *Populus*. *BMC Genomics* 11:129-129.
- Berlin S, Trybush SO, Fogelqvist J, Gyllenstrand N, Hallingbäck HR, Åhman I, Nordh NE, Shield I, Powers SJ, Weih M, et al. 2014. Genetic diversity, population structure and phenotypic variation in European *Salix viminalis* L. (Salicaceae). *Tree Genet Genomes* 10:1595-1610.
- Bolger AM, Lohse M, Usadel B. 2014. Trimmomatic: a flexible trimmer for Illumina sequence data. *Bioinformatics* 30:2114-2120.
- Boucher LD, Manchester SR, Judd WS. 2003. An extinct genus of Salicaceae based on twigs with attached flowers, fruits, and foliage from the Eocene Green River Formation of Utah and Colorado, USA. *Am J Bot* 90:1389-1399.
- Bull JJ. 1983. Evolution of sex determining mechanisms: Benjamin/Cummings Pub. Co.
- Carvalho AB, Dobo BA, Vibranovski MD, Clark AG. 2001. Identification of five new genes on the Y chromosome of *Drosophila melanogaster*. *Proc Natl Acad Sci U S A* 98:13225-13230.
- Charlesworth B. 1996. The evolution of chromosomal sex determination and dosage compensation. *Curr Biol* 6:149-162.
- Charlesworth B, Coyne JA, Barton NH. 1987. The relative rates of evolution of sex-chromosomes and autosomes. *American Naturalist* 130:113-146.
- Charlesworth D. 2016. Plant sex chromosomes. *Annu Rev Plant Biol* 67:397-420.
- Connallon T, Knowles LL. 2005. Intergenomic conflict revealed by patterns of sex-biased gene expression. *Trends Genet* 21:495-499.
- Cronk QC, Needham I, Rudall PJ. 2015. Evolution of catkins: Inflorescence morphology of selected Salicaceae in an evolutionary and developmental context. *Front Plant Sci* 6:1030.
- Darlington CD, Wylie AP. 1955. Chromosome atlas of flowering plants: Allen & Unwin.
- Emerson JJ, Kaessmann H, Betran E, Long M. 2004. Extensive gene traffic on the mammalian X chromosome. *Science* 303:537-540.
- Fisher RA. 1931. The evolution of dominance. *Biol Rev* 6:345-368.

- Fujii T, Shimada T. 2007. Sex determination in the silkworm, *Bombyx mori*: A female determinant on the W chromosome and the sex-determining gene cascade. *Semin Cell Dev Biol* 18:379-388.
- Gaudet M, Jorge V, Paolucci I, Beritognolo I, Mugnozza GS, Sabatti M. 2008. Genetic linkage maps of *Populus nigra* L. including AFLPs, SSRs, SNPs, and sex trait. *Tree Genet Genomes* 4:25-36.
- Geraldes A, Hefer CA, Capron A, Kolosova N, Martinez-Nuñez F, Soolanayakanahally RY, Stanton B, Guy RD, Mansfield SD, Douglas CJ, et al. 2015. Recent Y chromosome divergence despite ancient origin of dioecy in poplars (*Populus*). *Mol Ecol* 24:3243-3256.
- Goodfellow PN, Lovell-Badge R. 1993. *SRY* and Sex determination in mammals. *Annu Rev Genet* 27:71-92.
- Hallingbäck HR, Fogelqvist J, Powers SJ, Turrión-Gómez J, Rossiter R, Amey J, Martin T, Weih M, Gyllenstrand N, Karp A, et al. 2016. Association mapping in *Salix viminalis* L. (Salicaceae) - identification of candidate genes associated with growth and phenology. *GCB Bioenergy* 8:670-685.
- Handley LJL, Ceplitis H, Ellegren H. 2004. Evolutionary strata on the chicken Z chromosome: Implications for sex chromosome evolution. *Genetics* 167:367-376.
- Hodgkin J. 1990. Sex determination compared in *Drosophila* and *Caenorhabditis*. *Nature* 344:721-728.
- Hou J, Ye N, Dong Z, Lu M, Li L, Yin T. 2016. Major chromosomal rearrangements distinguish willow and poplar after the ancestral “Salicoid” genome duplication. *Genome Biol Evol* 8:1868-1875.
- Hou J, Ye N, Zhang D, Chen Y, Fang L, Dai X, Yin T. 2015. Different autosomes evolved into sex chromosomes in the sister genera of *Salix* and *Populus*. *Sci Rep* 5:9076.
- Hough J, Hollister JD, Wang W, Barrett SCH, Wright SI. 2014. Genetic degeneration of old and young Y chromosomes in the flowering plant *Rumex hastatulus*. *Proc Natl Acad Sci U S A* 111:7713-7718.
- Jaquiéry J, Rispe C, Roze D, Legeai F, Le Trionnaire G, Stoeckel S, Mieuzet L, Da Silva C, Poulain J, Prunier-Leterme N, et al. 2013. Masculinization of the X chromosome in the pea aphid. *PLoS Genet* 9:e1003690.

- Kersten B, Pakull B, Fladung M. 2012. Mapping of the sex trait and sequence analysis of two linked genomic regions in *Populus tremuloides*. ScienceMed 3:203-210.
- Kersten B, Pakull B, Groppe K, Lueneburg J, Fladung M. 2014. The sex-linked region in *Populus tremuloides* Turesson 141 corresponds to a pericentromeric region of about two million base pairs on *P. trichocarpa* chromosome 19. Plant Biol (Stuttg) 16:1-8.
- Kim D, Pertea G, Trapnell C, Pimentel H, Kelley R, Salzberg SL. 2013. TopHat2: accurate alignment of transcriptomes in the presence of insertions, deletions and gene fusions. Genome Biol 14:R36-R36.
- Lahn BT, Page DC. 1997. Functional coherence of the human Y chromosome. Science 278:675-680.
- Langmead B, Trapnell C, Pop M, Salzberg SL. 2009. Ultrafast and memory-efficient alignment of short DNA sequences to the human genome. Genome Biol 10:R25.
- Li H. 2013. Aligning sequence reads, clone sequences and assembly contigs with BWA-MEM. arXiv preprint.
- Li H, Handsaker B, Wysoker A, Fennell T, Ruan J, Homer N, Marth G, Abecasis G, Durbin R. 2009. The Sequence Alignment/Map format and SAMtools. Bioinformatics 25:2078-2079.
- Li R, Zhu H, Ruan J, Qian W, Fang X, Shi Z, Li Y, Li S, Shan G, Kristiansen K, et al. 2010. *De novo* assembly of human genomes with massively parallel short read sequencing. Genome Res 20:265-272.
- Löytynoja A. 2014. Phylogeny-aware alignment with PRANK. Methods Mol Biol 1079:155-170.
- Manchester SR, Judd WS, Handley B. 2006. Foliage and fruits of early Poplars (Salicaceae: *Populus*) from the Eocene of Utah, Colorado, and Wyoming. Int J Plant Sci 167:897-908.
- Mank JE. 2017. The transcriptional architecture of phenotypic dimorphism. Nature Ecol Evol (in press).
- Mank JE, Avise JC. 2009. Evolutionary diversity and turn-over of sex determination in teleost fishes. Sex Dev 3:60-67.
- Mank JE, Axelsson E, Ellegren H. 2007a. Fast-X on the Z: Rapid evolution of sex-linked genes in birds. Genome Res 17:618-624.

- Mank JE, Hultin-Rosenberg L, Axelsson E, Ellegren H. 2007b. Rapid evolution of female-biased, but not male-biased, genes expressed in the avian brain. *Mol Biol Evol* 24:2698-2706.
- Mank JE, Vicoso B, Berlin S, Charlesworth B. 2010. Effective population size and the Faster-X effect: Empirical results and their interpretation. *Evolution* 64:663-674.
- Marcais G, Kingsford C. 2011. A fast, lock-free approach for efficient parallel counting of occurrences of k-mers. *Bioinformatics* 27:764-770.
- Marchler-Bauer A, Derbyshire MK, Gonzales NR, Lu S, Chitsaz F, Geer LY, Geer RC, He J, Gwadz M, Hurwitz DI, et al. 2015. CDD: NCBI's conserved domain database. *Nucleic Acids Res* 43:D222-D226.
- Martin M. 2011. Cutadapt removes adapter sequences from high-throughput sequencing reads. *EMBnetjournal* 17:10-10.
- Meisel RP, Connallon T. 2013. The faster-X effect: integrating theory and data. *Trends Genet* 29:537-544.
- Miura I. 2008. An evolutionary witness: The frog *Rana rugosa* underwent change of heterogametic sex from XY male to ZW female. *Sex Dev* 1:323-331.
- Moghadam HK, Pointer MA, Wright AE, Berlin S, Mank JE. 2012. W chromosome expression responds to female-specific selection. *Proc Natl Acad Sci U S A* 109:8207-8211.
- Pakull B, Groppe K, Meyer M, Markussen T, Fladung M. 2009. Genetic linkage mapping in aspen (*Populus tremula* L. and *Populus tremuloides* Michx.). *Tree Genet Genomes* 5:505-515.
- Paolucci I, Gaudet M, Jorge V, Beritognolo I, Terzoli S, Kuzminsky E, Muleo R, Scarascia Mugnozza G, Sabatti M. 2010. Genetic linkage maps of *Populus alba* L. and comparative mapping analysis of sex determination across *Populus* species. *Tree Genet Genomes* 6:863-875.
- Papadopoulos AST, Chester M, Ridout K, Filatov DA. 2015. Rapid Y degeneration and dosage compensation in plant sex chromosomes. *Proc Natl Acad Sci U S A* 112:13021-13026.
- Parisi M. 2003. Paucity of genes on the *Drosophila* X chromosome showing male-biased expression. *Science* 299:697-700.

- Phillips RB, Konkol NR, Reed KM, Stein JD. 2001. Chromosome painting supports lack of homology among sex chromosomes in *Oncorhynchus*, *Salmo*, and *Salvelinus* (Salmonidae). *Genetica* 111:119-123.
- Pucholt P, Hallingbäck HR, Berlin S. 2017. Allelic incompatibility can explain female biased sex ratios in dioecious plants. *BMC Genomics* 18:251.
- Pucholt P, Rönnberg-Wästljung AC, Berlin S. 2015. Single locus sex determination and female heterogamety in the basket willow (*Salix viminalis* L.). *Heredity* 114:575-583.
- Qiu S, Bergero R, Charlesworth D. 2013. Testing for the footprint of sexually antagonistic polymorphisms in the pseudoautosomal region of a plant sex chromosome pair. *Genetics* 194:663-672.
- Quinlan AR, Hall IM. 2010. BEDTools: A flexible suite of utilities for comparing genomic features. *Bioinformatics* 26:841-842.
- Rice WR. 1984. Sex chromosomes and the evolution of sexual dimorphism. *Evolution* 38:735-742.
- Rice WR. 1996. Evolution of the Y sex chromosome in animals. *Bioscience* 46:331-343.
- Sackton TB, Corbett-Detig RB, Nagaraju J, Vaishna L, Arunkumar KP, Hartl DL. 2014. Positive selection drives Faster-Z evolution in Silkmoths. *Evolution* 68:2331-2342.
- Smith CA, Roeszler KN, Ohnesorg T, Cummins DM, Farlie PG, Doran TJ, Sinclair AH. 2009. The avian Z-linked gene *DMRT1* is required for male sex determination in the chicken. *Nature* 461:267-271.
- Song L, Florea L. 2015. Rcorrector: efficient and accurate error correction for Illumina RNA-seq reads. *GigaScience* 4:48.
- Song L, Florea L, Langmead B. 2014. Lighter: fast and memory-efficient sequencing error correction without counting. *Genome Biol* 15:509.
- Spigler RB, Lewers KS, Main DS, Ashman TL. 2008. Genetic mapping of sex determination in a wild strawberry, *Fragaria virginiana*, reveals earliest form of sex chromosome. *Heredity* 101:507-517.
- Stöck M, Horn A, Grossen C, Lindtke D, Sermier R, Betto-Colliard C, Dufresnes C, Bonjour E, Dumas Z, Luquet E, et al. 2011. Ever-young sex chromosomes in European tree frogs. *PLoS Biol* 9:e1001062.

- Telgmann-Rauber A, Jamsari A, Kinney MS, Pires JC, Jung C. 2007. Genetic and physical maps around the sex-determining M-locus of the dioecious plant asparagus. *Mol Genet Genomics* 278:221-234.
- Tennesen JA, Govindarajulu R, Liston A, Ashman T-L. 2016. Homomorphic ZW chromosomes in a wild strawberry show distinctive recombination heterogeneity but a small sex-determining region. *New Phytol* 211:1412-1423.
- Trapnell C, Williams Ba, Pertea G, Mortazavi A, Kwan G, van Baren MJ, Salzberg SL, Wold BJ, Pachter L. 2010. Transcript assembly and quantification by RNA-Seq reveals unannotated transcripts and isoform switching during cell differentiation. *Nat Biotechnol* 28:511-515.
- Tuskan GA, Difazio S, Jansson S, Bohlmann J, Grigoriev I, Hellsten U, Putnam N, Ralph S, Rombauts S, Salamov A, et al. 2006. The genome of black cottonwood, *Populus trichocarpa* (Torr. & Gray). *Science* 313:1596-1604.
- Vicoso B, Bachtrog D. 2015. Numerous transitions of sex chromosomes in Diptera. *PLoS Biol* 13:e1002078.
- Vicoso B, Emerson JJ, Zektser Y, Mahajan S, Bachtrog D. 2013a. Comparative sex chromosome genomics in snakes: Differentiation, evolutionary strata, and lack of global dosage compensation. *PLoS Biol* 11:e1001643.
- Vicoso B, Kaiser VB, Bachtrog D. 2013b. Sex-biased gene expression at homomorphic sex chromosomes in emus and its implication for sex chromosome evolution. *Proc Natl Acad Sci U S A* 110:6453-6458.
- Wang J, Na J-K, Yu Q, Gschwend AR, Han J, Zeng F, Aryal R, VanBuren R, Murray JE, Zhang W, et al. 2012. Sequencing papaya X and Y<sup>h</sup> chromosomes reveals molecular basis of incipient sex chromosome evolution. *Proc Natl Acad Sci U S A* 109:13710-13715.
- Wang Z, Zhang J, Yang W, An N, Zhang P, Zhang G, Zhou Q. 2014. Temporal genomic evolution of bird sex chromosomes. *BMC Evol Biol* 14:250.
- Wright AE, Harrison PW, Zimmer F, Montgomery SH, Pointer MA, Mank JE. 2015. Variation in promiscuity and sexual selection drives avian rate of Faster-Z evolution. *Mol Ecol* 24:1218-1235.
- Wright AE, Moghadam HK, Mank JE. 2012. Trade-off between selection for dosage compensation and masculinization on the avian Z chromosome. *Genetics* 192:1433-1445.

- Yang X, Schadt EE, Wang S, Wang H, Arnold AP, Ingram-Drake L, Drake TA, Lusis AJ. 2006. Tissue-specific expression and regulation of sexually dimorphic genes in mice. *Genome Res* 16:995-1004.
- Yang Z. 2007. PAML 4: phylogenetic analysis by maximum likelihood. *Mol Biol Evol* 24:1586-1591.
- Yazdi HP, Ellegren H. 2014. Old but not (so) degenerated - Slow evolution of largely homomorphic sex chromosomes in ratites. *Mol Biol Evol* 31:1444-1453.
- Yin T, DiFazio SP, Gunter LE, Zhang X, Sewell MM, Woolbright SA, Allan GJ, Kelleher CT, Douglas CJ, Wang M, et al. 2008. Genome structure and emerging evidence of an incipient sex chromosome in *Populus*. *Genome Res* 18:422-430.
- Zhou Q, Bachtrog D. 2012. Chromosome-wide gene silencing initiates Y degeneration in *Drosophila*. *Curr Biol* 22:522-525.

**Table 1. P<sub>i</sub>S for males and females for the sex chromosomes of *S. viminalis*.**

Region	Genes	Female p <sub>i</sub> S (95% CI)	Male p <sub>i</sub> S (95% CI)
SD region	72	0.0098 (0.0056-0.0155)	0.0053 (0.0017-0.0117)
Autosomes	8868	0.0101 <sup>1</sup> (0.0097-0.0105)	0.0087 <sup>1</sup> (0.0083-0.0091)

<sup>1</sup> Higher female autosomal p<sub>i</sub>s is due to greater average heterozygosity in female compared to male samples. This likely results in an overestimate of sex chromosome divergence.

## Figure legends

Figure 1. Phylogeny showing the relative divergence times of the evolution of dioecy and the sex chromosomes as well as the lineage split between poplars and willows.

Figure 2. Genome-wide analysis of patterns of sequence divergence. The innermost circle (A) displays the association (as Bonferroni corrected *p*-values of a Fisher's exact test) of genetic SNP markers with the sex of the individual based on a bi-parental population of 271 offspring individuals (Pucholt, et al. 2017). The second circle (B) displays the relative Log<sub>2</sub> female:male genome coverage, while the outermost circle (C) displays the Log<sub>2</sub> absolute female (red) and male (blue) SNP density. The region on chromosome 15 with genetic markers strongly associated with phenotypic sex is highlighted throughout all circles. The lines represent a moving average over a window size of 25 scaffolds/markers.

Figure 3. Patterns of sex chromosome differentiation on chromosome 15. (A) Log<sub>2</sub> normalized per base coverage of all individuals that were used in the study (red: females, blue: males). (B) Log<sub>10</sub> female:male SNP density. (C) Log<sub>2</sub> female:male FPKM expression values in catkins. (D) Log<sub>2</sub> female:male FPKM expression values in leaves. Shaded areas represent the bootstrap based 95% confidence interval, horizontal dashed lines represent the bootstrap median value while solid lines represent a moving average over a window size of 25 scaffolds/genes for the metrics in question. Grey vertical dashed lines represent the border of the SD region as defined by the SNP analysis.

Figure 4. Heatmap of FPKM values of genes that show sex biased expression in at least one tissue ( $q < 0.05$ ;  $\log_2 FC > 1$ ) and that are expressed with an average FPKM value of  $> 1$ . Samples were clustered using hierarchical cluster analysis (top). Red: female tissue, Blue: male tissue.



## Figures

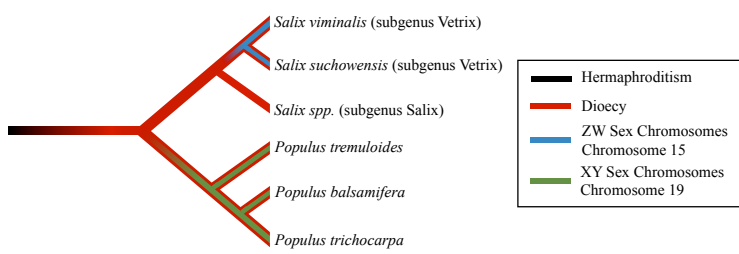


Figure 1

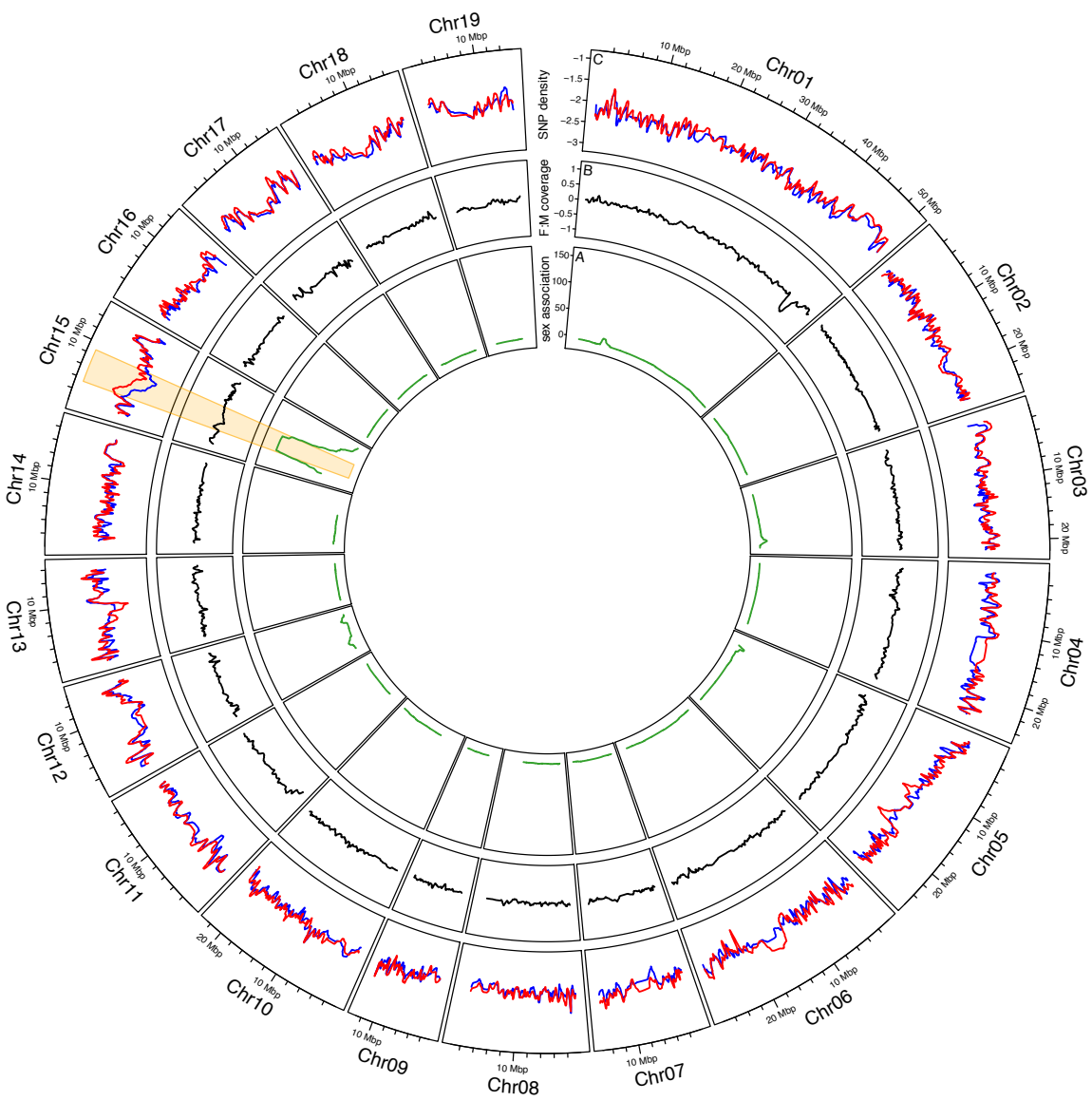


Figure 2

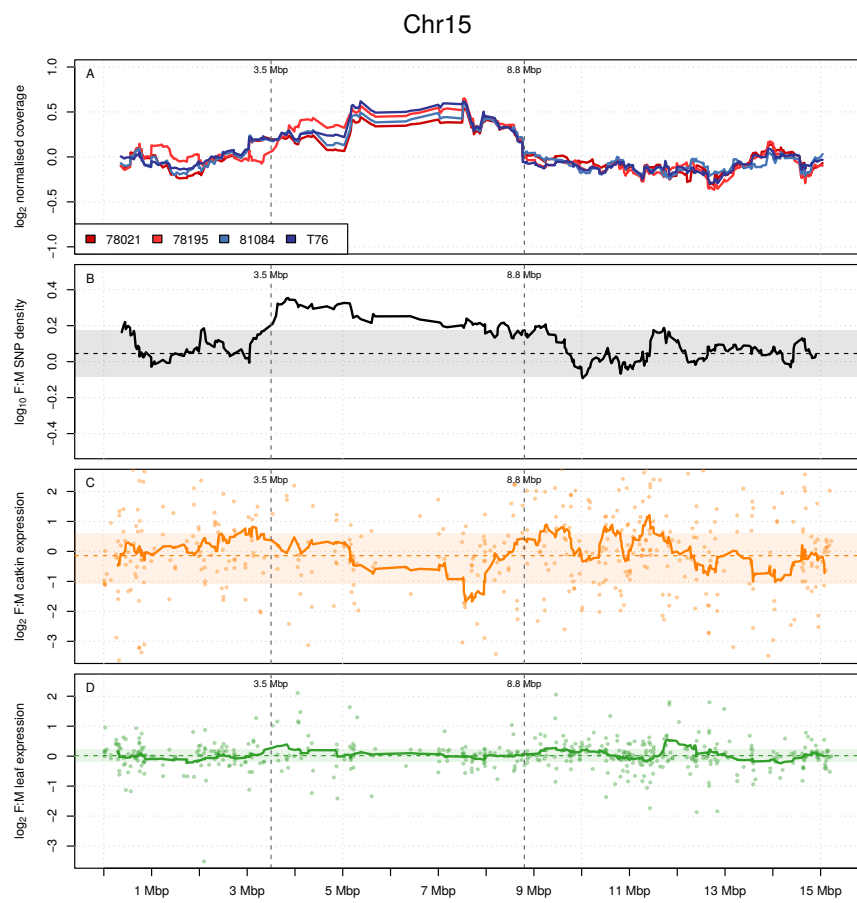


Figure 3

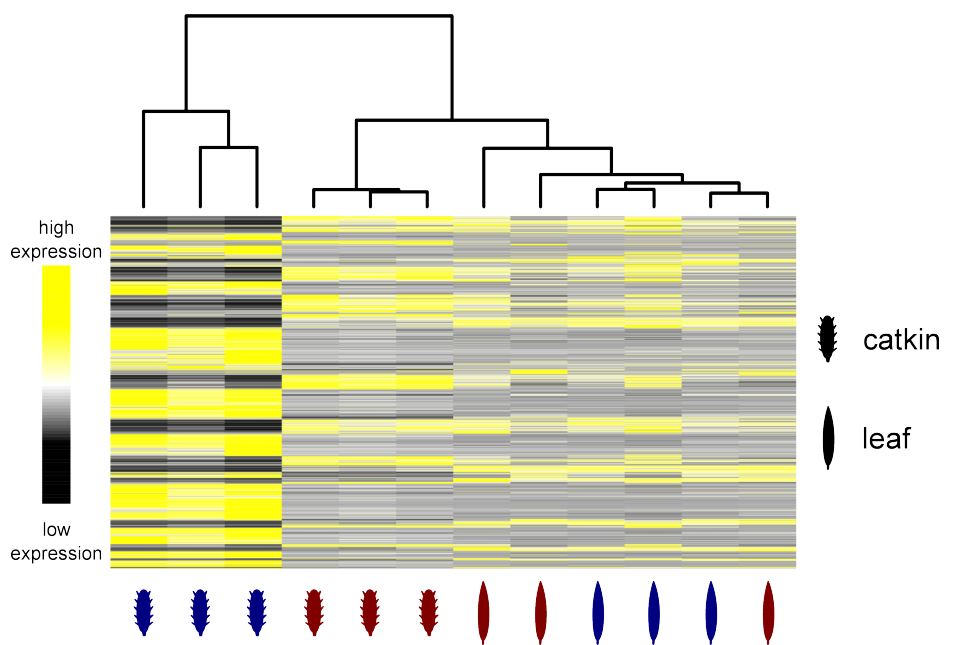


Figure 4